

Video Enhancement Based on A Robust Hampel Iterative SRR with a General Observation Model

Vorapoj Patanavijit¹,

Supatana Auethavekiat², and Somchai Jitapunkul³, Non-members

ABSTRACT

This paper proposes a novel robust Super-Resolution Reconstruction (SRR) framework that can enhance a real complex video sequence and is applicable to any noise models. Although SRR algorithms have received considerable attention within the traditional research community, these algorithms are typically very sensitive to their assumed model of data and noise, which limits their utility. The real noise models that corrupt the measured sequence are unknown; consequently, SRR algorithms using L1 or L2 norm may degrade the image sequence rather than enhance it therefore the robust norm applicable to several noise and data models is desired in SRR algorithms. This paper proposes a SRR framework based on the stochastic regularization technique of Bayesian MAP estimation by minimizing a cost function. In order to tolerate to any noise models, the Hampel norm is used for measuring the difference between the projected estimate of the high-resolution image and each low resolution image, and removing outliers in the data. Tikhonov regularization is used to remove artifacts from the final result and improve the rate of convergence. Moreover, in order to cope with real video sequences and complex motion sequences, this paper proposes a SRR General Observation Model (GOM or affine block-based transform) devoted to the case of nonisometric inter-frame motion. In the experimental section, the proposed framework can enhance real complex motion sequences, such as Suzie and Foreman sequence, and confirm the effectiveness of our algorithm and demonstrate its superiority to other SRR algorithms based on L1 and L2 norm for several noise models (such as AWGN, Poisson noise, Salt & Pepper noise and Speckle noise) at several noise power.

Keywords: SRR (Super Resolution Reconstruction), Digital Image Reconstruction, ML Regularization

1. GENERAL INTRODUCTION

Several distorting processes affect the quality of image sequences or video acquired by commercial digital cameras. Some of the more important distorting effects are warping, blurring, down sampling and additive noise. The term SRR [1, 2] ranges from blur removal by deconvolution in single image to the creation of a single HR (High Resolution) image from multiple LR (Low Resolution) images having relative sub-pixel displacements. In all cases, the goal of SRR is to remove the effect of blurring and noise in the LR images and to obtain images with resolutions that go beyond the conventional limits of the uncompensated imaging system. Thus, the major advantage of this approach is that the cost of implementation is reduced and the existing low resolution (LR) imaging systems can still be utilized. Therefore, SRR applications on image sequences grow rapidly as the theory gains exposure. Continuing researches and the availability of fast computational machineries have made these methods increasingly attractive in applications requiring the highest restoration performance. SRR techniques have already been applied to problems in a number of applications such as satellite imaging, astronomical imaging, video enhancement and restoration, video standards conversion, confocal microscopy, digital mosaicing, aperture displacement cameras, medical imaging, diffraction tomography and video freeze frame. In SRR, typically, the LR images represent different “looks” at the same scene [2] hence LR images are sub-sampled (aliased) as well as shifted with sub-pixel precision. If the LR images are shifted by integer units, then each image contains the same information, and thus there is no new information that can be used to reconstruct a HR image. If the LR images have different sub-pixel shifts from each other and aliasing is present, however, then each

This work has been supported by Research Grant (MRG5180263) for New Scholar from TRF (Thai Research Fund) and CHE (Commission on Higher Education) under Assumption University (Thailand).

¹ The author is with Department of Computer and Network Engineering, Faculty of Engineering, Assumption University, Bangkok, Thailand, Email: Patanavijit@yahoo.com

^{2,3} The authors are with Department of Electrical Engineering, Faculty of Engineering, Chulalongkorn University, Bangkok, Thailand, Email: Asupatana@yahoo.com and Somchai.j@chula.ac.th

image cannot be obtained from others. In this case, the new information contained in each LR image can be exploited to obtain a HR image. To obtain different looks of the same scene, some relative scene motions must exist from frame to frame via multiple scenes or video sequences. Multiple scenes can be obtained from one camera with several captures or from multiple cameras located in different positions. These scene motions can occur due to the controlled motions in imaging systems, e.g., images acquired from orbiting satellites. The same is true for uncontrolled motions, e.g., movement of local objects or vibrating imaging systems. If these scene motions are known or can be estimated within sub-pixel accuracy and we combine these LR images then SRR is possible.

The SRR problem is modelled by using sparse matrices and analyzed from many reconstruction methods such as the non-uniform interpolation, frequency domain, Maximum-Likelihood (ML), Maximum A-Posteriori (MAP), and Projection Onto Convex Sets (POCS). For comprehensive review in SRR algorithm in the last two decades refer to our previous work in [3].

In this section, we first study and review some of the previous works on SRR algorithm regarding for SRR estimation techniques. Later, the SRR Classical Observation Models (COM) are reviewed. Finally, we show the inefficiency of independent solutions for these problems and discuss the obstacles to designing a unified framework to enhance image sequences or video.

1.1 Observation Model in SRR

This section reviews the literature from the registration point of view because the quality of the SR (super-resolution) image depends heavily on the accuracy of the observation model. Subpixel precision in the motion field is needed to achieve the desired improvement.

Most SRR algorithms reviewed in [3] are restricted to globally or locally uniform translational displacement between the measured images or sequences. This implies that the measured images or sequences are observed at a high temporal frequency sampling (or high frame rate) but the measured images or sequences are usually observed by the real commercial cameras at low temporal frequency sampling (or low frame rate) such as standard sequences (Foreman, Carphone, Susie, etc.). The measured images or sequences have many complex motions instead of only a simple translational motion; therefore, the pure translation model can not effectively represent the real complex motion and SRR applications can be applied only on the sequences that have simple translation motion as shown in [4]. In [3-4], we proposed the SRR using a regularized ML estimator with affine block-based registration for the real image sequence. G. Rochefort et al. [5] proposed SRR approach based

on regularized ML for the extended original observation model [6,7] devoted to the case of nonisometric inter-frame motion such as affine motion in 2006. This paper proposed the novel general SRR observation model to overcome the insufficient temporal sampling frequency and to model the real complex motion sequence that the SRR COM model can not support. To implement the proposed SRR observation model, the sub-pixel image registration is designed to calculate the nonisometric inter-frame motion parameter. Moreover, the fast algorithm is proposed to reduce the computational load for the proposed sub-pixel registration.

1.2 SRR Estimation Technique in SRR

In this section, the relevant research papers, published in the conferences and journals, are comprehensively reviewed from the estimation point of view because the SRR estimation is one of the most crucial parts of the SRR research areas and directly impact to the SRR performance.

The early SRR algorithms [7-12] are based on classical ML technique using L2 norm with several regularized functions such as GGMRF (General Gaussian Markov Random Field) [13], HMRF (Huber Markov Random Field) [8-9] and BTV (Bilateral Total Variance) [14], etc. Later, the SRR algorithms [15-18] based on L1 norm have been proposed since 2004.

For the cost function for the data fidelity, all the SRR algorithms [1-18] are based on the simple estimation techniques such as L1 norm or L2 norm minimization. Therefore, these SRR methods are very sensitive to their assumed data and noise models. The success of SRR algorithm is highly dependent on the model accuracy regarding the imaging process. These models do not always represent the actual imaging process, as they are merely mathematically convenient formulations of some general prior information. When the data or noise model assumptions do not faithfully describe the measure data, the estimator performance degrades. Furthermore, the existence of outliers defined as data points with different distributional characteristics than the assumed model will produce erroneous estimates. Most noise models used in SRR algorithm are based on AWGN model at low power; therefore, SRR algorithms can be effectively applied only on the image sequence that is corrupted by AWGN. Only with this AWGN model, L1 norm or L2 (quadratic) norm error are effective. For normal distributed data, the L1 norm produces estimates with higher variance than the optimal L2 norm. On the other hand the L2 norm is very sensitive to outliers and noise because the influence function increases linearly and without bound. The real noise models that corrupt the measured sequence are unknown; consequently, SRR algorithm using L1 norm or L2 norm may degrade the image sequence rather than enhance it. Therefore, the robust norm which is

applicable to several noise and data models is desired in SRR algorithms. From the robust statistical estimation study [19-20], Hampel Norm [21-23] is more robust than L1 and L2. Hampel Norm is also capable of outlier rejection and more forgiving on outliers; that is, the error is increased less rapidly than L2. Consequence, we used to propose a robust iterative SRR algorithm based on Hampel norm that can be applied on simple translation motion sequence [23]. This paper proposed the novel robust SRR framework that can be applied not only on any noise models but also applied on complex motion sequences. The algorithm is based on the iterative robust SRR algorithm using the stochastic regularization technique of Bayesian MAP estimation by minimizing a cost function. The Hampel Norm is used for measuring the difference between the projected estimation of the high-resolution image and each low resolution image, removing outliers in the data. Tikhonov regularization is used to remove artifacts from the final result and improve the rate of convergence. In order to cope with real sequences and complex motion sequences, this paper proposes the general SRR observation model by introducing the affine block-based transform, devoted to the case of nonisometric inter-frame motion.

The organization of this paper is as follows. Section 2 explains the main concepts of SRR algorithms in both observation model and estimation technique point of view. Section 3 introduces the iterative regularized SRR based on L1, L2 and Hampel with the proposed general observation model. Section 4 outlines the experimental results that are separated into two parts for comprehensive. First, the comparative results between the SRR algorithm based on Hampel, L1 and L2 norm with the classical observation model are presented. Later, the comparative results between the SRR algorithm using the proposed Hampel norm and the L1 and L2 norm with the proposed observation model are presented. The real complex motion sequences (such as Suzie and Foreman) are used in the experiment and several noise models (such as AWGN, Poisson noise, Salt & Pepper noise and Speckle noise) are used in the experiment. Finally, Section 5 provides the summary and conclusion.

2. SRR FRAMEWORK WITH CLASSICAL AND GENERAL OBSERVATION MODEL

The first step to reconstruct the SRR image is to formulate an observation model that relates the original HR image to the observed LR sequences. We present the observation model for the general SRR from image sequences. Based on the observation model, probabilistic SRR formulations and solutions such as ML (Maximum Likelihood) estimators provide a simple and effective way to incorporate various regularizing constraints. Regularization reduces the

visibility of artifacts created during the inversion process. Then, we can rewrite the definition of these ML estimators in the SRR context as the minimization problem.

2.1 Observation Model of SRR

2.1.1 The Classical Observation Model (COM) of SRR

This section presents the SRR COM. Define a low-resolution (LR) image sequence, $\{\underline{\mathbf{Y}}_k\}$, as our measured data (The size of the LR images is $N_1 \times N_2$ pixels). A HR image $\underline{\mathbf{X}}(qN_1 \times qN_2$ pixels) is estimated from the LR sequences, where q is an integer interpolation factor in both the horizontal and vertical directions. To reduce the computational complexity, each frame is separated into overlapping blocks (the shaded blocks in Fig. 1(a) and Fig. 1(b)).

For notation convenience, all overlapping blocks in a frame will be presented as a vector, ordered column-wise lexicographically. The overlapping block in LR frame is denoted by $\underline{\mathbf{Y}}_k \in \mathbb{R}^{M^2} (M^2 \times 1)$ and the overlapping blocked in HR frame is denoted by $\underline{\mathbf{X}} \in \mathbb{R}^{q^2 M^2} (L^2 \times 1 \text{ or } q^2 M^2 \times 1)$. We assume that the two images are related via the following equation

$$\underline{\mathbf{Y}}_k = D_k H_k F_{C,k} \underline{\mathbf{X}} + \underline{\mathbf{V}}_k ; k = 1, 2, \dots, N \quad (1.1)$$

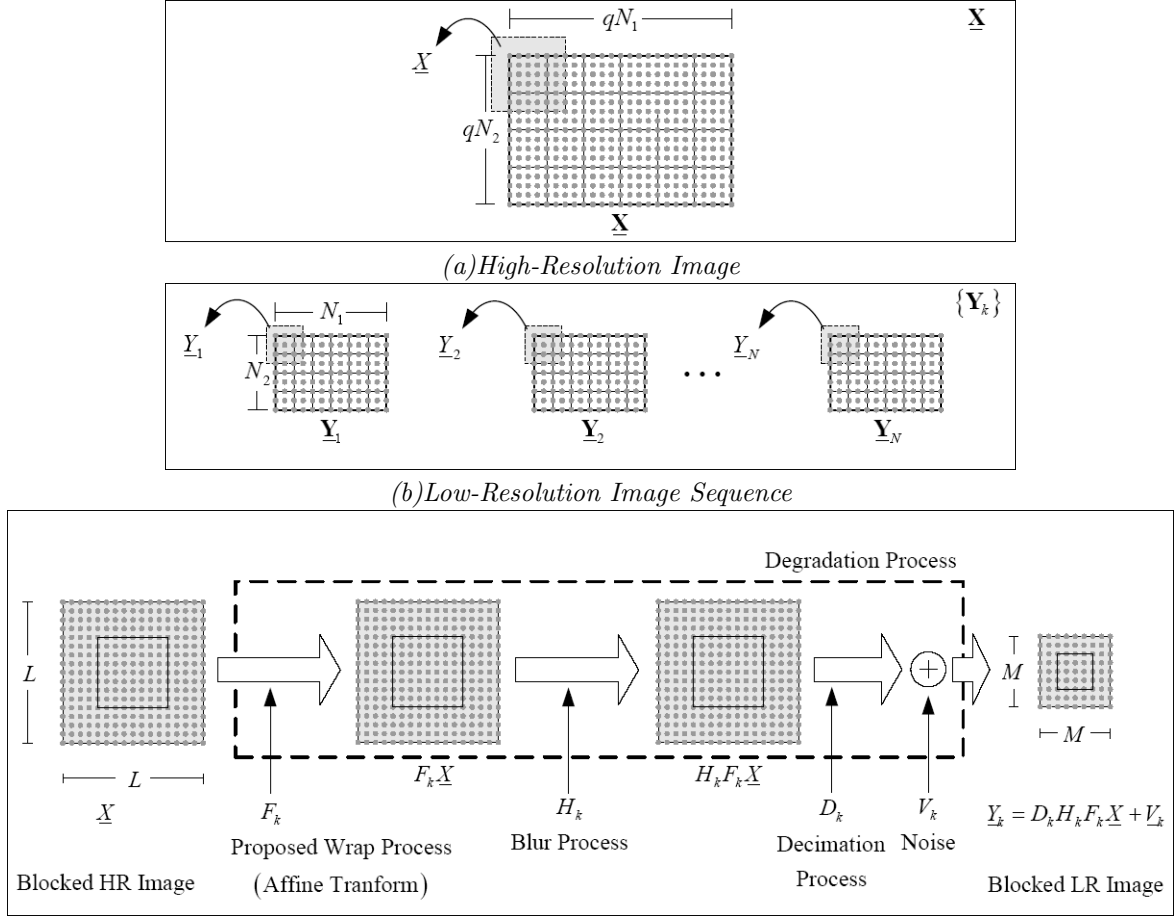
where $\underline{\mathbf{Y}}_k$ is a blurred, decimated, down sampled and contaminated by additive noise of $\underline{\mathbf{X}}$ (original overlapping HR image). The matrix $F_{C,k}$ ($F \in \mathbb{R}^{q^2 M^2 \times q^2 M^2}$) stands for the classical translation [9-14] between the images $\underline{\mathbf{X}}$ and $\underline{\mathbf{Y}}_k$. H_k is the blur matrix which is space and time invariant and $H_k \in \mathbb{R}^{q^2 M^2 \times q^2 M^2}$. D_k is the decimation matrix assumed constant and $D_k \in \mathbb{R}^{q^2 M^2 \times q^2 M^2}$. $\underline{\mathbf{V}}_k$ is a system noise and $\underline{\mathbf{V}}_k \in \mathbb{R}^{M^2}$.

2.1.2 The General Observation Model (GOM) of SRR

The pure translation model can not well represent the real complex motion effectively; therefore, the general observation model is desired. In this section, we first propose the general observation model for SRR algorithm based on stochastic regularization technique. From the high accuracy of the general observation model, the fast affine block-based registration [3-4] is used for registration step of SRR. Thus, we assume that the two images are related via the following equation (as shown in Fig. 1(c))

$$\underline{\mathbf{Y}}_k = D_k H_k F_k \underline{\mathbf{X}} + \underline{\mathbf{V}}_k ; k = 1, 2, \dots, N \quad (1.2)$$

where the matrix $F_k (F \in \mathbb{R}^{q^2 M^2 \times q^2 M^2})$ stands for the proposed nonisometric inter-frame warp [4] between the images $\underline{\mathbf{X}}$ and $\underline{\mathbf{Y}}_k$. The matrix F_k is created from affine motion vector but the matrix $F_{C,k}$



(c) The Relation between Overlapping Blocked HR Image and Overlapping Blocked LR Image Sequence

Fig.1: The General Observation Model (GOM)

in equation (1.1) is created from classical translation motion vector.

2.2 The Estimation Norm of SRR

Typically, many available estimators that estimate a HR image from a set of noisy LR images are not exclusively based on the LR measurement. They are also based on many assumptions such as noise or motion models and these models are not supposed to be accurate, as they are merely mathematically convenient formulations of some general prior information. When the fundamental assumptions of data and noise models do not faithfully describe the measured data, the estimator performance degrades. Moreover, existence of outliers defined as data points with different distributional characteristics than the assumed model will produce an error in estimation. Estimators promising optimality for a limited class of data and noise models may not be the most effective overall approach. Often, suboptimal estimation methods that are not as sensitive to modelling and data errors may produce better and more stable results; that is more robust.

A popular family estimator is the ML-type estima-

tor (ML estimators) [8-12]. We rewrite the definition of these estimators in the SRR framework as the following minimization problem:

$$\hat{\underline{X}} = \underset{\underline{X}}{\text{ArgMin}} \left\{ \sum_{k=1}^N \rho(D_k H_k F_k \underline{X} - \underline{Y}_k) \right\} \quad (2)$$

where $\rho(\cdot)$ is a error norm and $\hat{\underline{X}}$ is an estimated overlapping HR image. To minimize (2), the intensity at each pixel of the expected image must be close to those of original image.

2.2.1 L1 Norm Estimator

One of the popular robust estimators in SRR problem is the L1 norm estimators ($\rho(x) = \|x\|$) [16-18]. We rewrite the definition of these estimators in the SRR context as the following minimization problem:

$$\hat{\underline{X}} = \underset{\underline{X}}{\text{ArgMin}} \left\{ \sum_{k=1}^N \|D_k H_k F_k \underline{X} - \underline{Y}_k\| \right\} \quad (3)$$

The L1 norm is not sensitive to outliers because the influence function, $\rho'(\cdot)$, is constant and bound

but the L1 norm produces an estimator with higher variance than the L2 (quadratic) norm.

2.2.2 L2 Norm Estimator

Another popular estimators in SRR problem is the L2 norm estimators [8-12]. We rewrite the definition of these estimators in the SRR context as the following minimization problem:

$$\hat{\underline{X}} = \underset{\underline{X}}{\text{ArgMin}} \left\{ \sum_{k=1}^N \|D_k H_k F_k \underline{X} - \underline{Y}_k\|_2^2 \right\} \quad (4)$$

The L2 norm produces estimator with lower variance than the L1 norm but the L2 norm is very sensitive to outliers because the influence function of L2 norm increases linearly and without bound.

2.2.3 Robust Norm Estimator [19-20]

A robust estimation is an estimated technique that is resistance to outliers. In SRR framework, outliers are measured images or corrupted images that are highly inconsistent with the original image. Outliers may arise from several reasons such as procedural measurement error, noise or inaccurate mathematical model. Outliers should be investigated carefully; therefore, we need to analyze the outlier in a way which minimizes their effect on the estimated model. L2 norm estimation is highly susceptible to even a small number of discordant observations or outliers. For L2 norm estimation, the influence of the outlier is much larger than the other measured data because L2 norm estimation increases the effect of the error quadratically. Consequently, the robustness of L2 norm estimation is poor.

Much can be improved if the influence is bounded in one way or another. This is exactly the general idea of applying a robust error norm. Instead of using the sum of squared differences as in (4), this error norm should be selected such that the influence of the data whose error level (x) is high (outlier) is ruled out. In addition, one would like to have a smooth influence function so that numerical minimization of (5) is not too difficult. The suitable choice (among other) is the Hampel error norm [19-20] that is defined in (6). We rewrite the definition of these estimators in the SRR context as the following minimization problem:

$$\hat{\underline{X}} = \underset{\underline{X}}{\text{ArgMin}} \left\{ \sum_{k=1}^N \rho_{HAMPSEL} (D_k H_k F_k \underline{X} - \underline{Y}_k) \right\} \quad (5)$$

$$\rho_{HAMPSEL}(x) = \begin{cases} x^2 & ; |x| \leq T \\ 2T|x| - T^2 & ; T < |x| \leq 2T \\ 4T^2 - (3T - |x|)^2 & ; 2T < |x| \leq 3T \\ 4T^2 & ; |x| > 3T \end{cases} \quad (6)$$

The parameter T is Hampel constant parameter that is a soft threshold value and $T \in [0, 255]$. For

values of x smaller than T , the function follows the L2 norm. For values larger than T , the function gets saturated. Consequently for small value of x , the derivative of $\rho_{HAMPSEL}(\cdot)$ is nearly a constant. But for large values of x (for outliers), it becomes nearly zero. Therefore, in a Gauss-Newton style of optimization, the Jacobian matrix is virtually zero for outliers. Only residuals that are about as large as T or smaller than that play a role.

From L1 and L2 norm estimation point of view, Hampel norm acts as an L1 norm when x is large and as an L2 norm when x is small (normal-distribute data) therefore Hampel norm acts as the suitable appropriate norm for the particular values of x .

3. THE PROPOSED ROBUST SRR FRAMEWORK WITH GENERAL OBSERVATION MODEL

This section proposes the iterative SRR algorithm using L1, L2 and Hampel norm minimization with regularization functions for the COM and proposed GOM, described in previous section. Typically, SRR is an inverse problem [10-12] thus the process of computing an inverse solution can be, and often is, extremely unstable in that a small change in measurement (such as noise) can lead to an enormous change in the estimated image (SR Image). Therefore, SRR is an ill-posed or ill-conditioned problem. An important point is that it is commonly possible to stabilize the inversion process by imposing additional constraints that bias the solution, a process that is generally referred to as regularization. Regularization is frequently essential to producing a usable solution to an otherwise intractable ill-posed or ill-conditioned inverse problem because regularization can help the algorithm to remove artifacts from the final answer and improve the rate of convergence.

A block diagram of the proposed iterative SRR framework is illustrated in Figure 2. The proposed SRR framework is the iterative process composed of 2 main parts: the estimation of the registration parameters and the estimation of HR image. First, the initialized SR image is determined by interpolating LR image (the reference image). Second, the registration parameters, which used to wrap all low resolution images and used in the image estimation process, are estimated from low resolution images (or observed sequences). Third, all LR images, the estimated SR image, all registration information, regularized information and initial SR image are used in the image estimation process to generate the estimated SR image.

3.1 SRR based on L1 Norm with General Observation Model (GOB)

Combined with the GOM, we propose the SRR based on L1 norm. A regularization term compensates the missing information with some general prior

information about the desirable HR solution, and is usually implemented as a penalty factor in the generalized minimization cost function. This estimator is defined in the SRR as follows:

$$\hat{\underline{X}} = \underset{\underline{X}}{\text{ArgMin}} \left\{ \sum_{k=1}^N \|D_k H_k F_k \underline{X} - \underline{Y}_k\|_1 + \lambda \cdot \|\Gamma \underline{X}\|_2^2 \right\} \quad (7)$$

where λ is a regularized parameter and $\lambda \in [0, 1]$. The classical and simplest Tikhonov regularization functions is the Laplacian regularization [16] where the Laplacian kernel is defined as

$$\Gamma = \frac{1}{8} [1 \ 1 \ 1; 1 \ -8 \ 1; 1 \ 1 \ 1] \quad (8)$$

By the steepest descent method, the solution of equation (7) is defined as follows.

$$\hat{\underline{X}}_{n+1} = \hat{\underline{X}}_n + \beta \cdot \left\{ \begin{array}{l} \sum_{k=-N}^N F_k^T H_k^T D_k^T \text{sign}(\underline{Y}_k - D_k H_k F_k \hat{\underline{X}}_n) \\ -(\lambda \cdot (\Gamma^T \Gamma) \hat{\underline{X}}_n) \end{array} \right\} \quad (9)$$

where β is a step-size of the steepest descent method and $\beta \in [0, 1]$.

3.2 SRR based on L2 Norm with General Observation Model (GOB)

Combined with the GOM, we propose the SRR based on L2 norm. This estimator is defined in the SRR context with the combination of the Laplacian regularization as follows:

$$\hat{\underline{X}} = \underset{\underline{X}}{\text{ArgMin}} \left\{ \sum_{k=1}^N \|D_k H_k F_k \underline{X} - \underline{Y}_k\|_2^2 + \lambda \cdot \|\Gamma \underline{X}\|_2^2 \right\} \quad (10)$$

By the steepest descent method, the solution of equation (10) is defined as

$$\hat{\underline{X}}_{n+1} = \hat{\underline{X}}_n + \beta \cdot \left\{ \sum_{k=1}^N F_k^T H_k^T D_k^T (\underline{Y}_k - D_k H_k F_k \hat{\underline{X}}_n) - (\lambda \cdot (\Gamma^T \Gamma) \hat{\underline{X}}_n) \right\} \quad (11)$$

3.3 SRR based on Hampel Norm with General Observation Model (GOB)

Combined with the GOM, this paper proposes SRR using Hampel norm that is more robust than L1 and L2 norm. The definition of this estimator is defined in the SRR context as the following minimization problem:

$$\hat{\underline{X}} = \underset{\underline{X}}{\text{ArgMin}} \left\{ \sum_{k=1}^N f_{HAMP\acute{E}L} \|D_k H_k F_k \underline{X} - \underline{Y}_k\| + \lambda \cdot \|\Gamma \underline{X}\|_2^2 \right\} \quad (12)$$

By the steepest descent method, the solution of equation (12) is defined as

$$\hat{\underline{X}}_{n+1} = \hat{\underline{X}}_n + \beta \cdot \left\{ \sum_{k=1}^N F_k^T H_k^T D_k^T \psi_{HAMP\acute{E}L}(\underline{Y}_k - D_k H_k F_k \hat{\underline{X}}_n) - (\lambda \cdot (\Gamma^T \Gamma) \hat{\underline{X}}_n) \right\} \quad (13-1)$$

$$\psi_{HAMP\acute{E}L}(x) = f'_{HAMP\acute{E}L}(x)$$

$$= \begin{cases} x^2 & ; |x| \leq T \\ 2T|x| - T^2 & ; T < |x| \leq 2T \\ 4T^2 - (3T - |x|)^2 & ; 2T < |x| \leq 3T \\ 4T^2 & ; |x| > 3T \end{cases} \quad (13-2)$$

3.4 The Proposed Registration for General Observation Model (GOB) of SRR [3-4]

The assumption of the SRR COM that only translation motion exists in a sequence limits the SRR to the sequences that have simple translation motion; hence, the registration is simple. Only 2 motion parameters need to be estimated for the translation motion and the registration parameters defined in (14) (2 motion parameters per block) for the translation is easily estimated because several registration estimation techniques have been proposed such as FS (Full Search), 3SS (3 Step Search) or DS (Diamond Search).

$$mv_{x,tran}(x, y) = a \text{ and } mv_{y,tran}(x, y) = b \quad (14)$$

This equation means that every pixel (in an image block) can only move in the same direction. From the proposed iterative SSR framework illustrated in Figure 2, the registration parameters for the GOM (6 motion parameters per block) must be calculated as defined in (15) for image fusion process; therefore, a high accuracy registration algorithm is desired for the proposed SRR framework.

$$mv_{x,affine}(x, y) = ax + by + c \quad (15.1)$$

$$mv_{y,affine}(x, y) = dx + ey + f \quad (15.2)$$

This equation means that each pixel (in an image block) can move in the different directions. In this section, we propose a scheme for estimating affine block-based motion vectors for registration step. The estimation can be separated into 2 stages. In the first

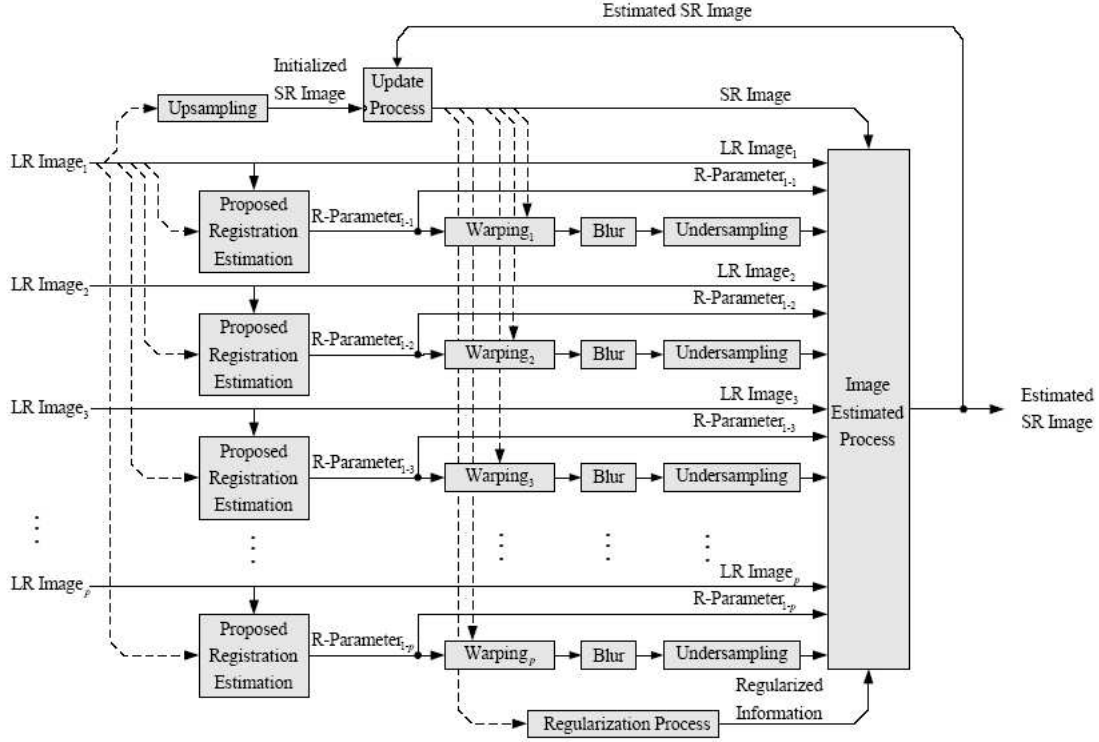


Fig.2: The Proposed Super-Resolution Reconstruction Framework

stage of the estimation algorithm, the current and reference frames are divided into 50% overlapping blocks (16×16). This stage divides the image into small areas in order to detect and estimate the local motions. The advantage of the block processing is the reduction of the computational load and the possibility of parallel processing. In the second stage, the affine motion vector of each block between the current and reference frame is computed by the M3SS (Modified Three Step Search). The M3SS is proposed to reduce a very high computational load in affine motion vector estimation. The M3SS is designed based on the popular 3SS (Three Step Search). The 3SS (Three Step Search) is one of the popular and fast algorithms used in the translational registration; therefore, this paper develops the M3SS (6 motion parameter estimation) based on 3SS (2 motion parameter estimation).

For the 7×7 displacement window (translational deformation) and degree (rotation, extraction or expansion deformation), the proposed M3SS algorithm utilizes a search pattern with $3^6 = 729$ check points (the parameters vary in 6 dimensions instead of 2 dimensions as in 3SS check points) on a search window in the first step. The set of parameters having the minimum error is used as the center of the search area in the subsequent step. The search window is reduced by half in the subsequent step until the search window equals to the pre-determined resolution. The criterion for parameter selection in this paper was based on experiments and the chosen parameters produce

the highest PSNR result on 3 standard sequences: Foreman, Carphone and Stefan [3-4]. The process of M3SS is used in the following description:

Step 1 : Initialize the dimension of the searching area to the value depicted in (16).

$$[a, b, c, d, e, f] = [\pm 0.16, \pm 0.16, \pm 2, \pm 0.16, \pm 0.16, \pm 2] (16)$$

Step 2 : A minimum BDM (Block Distortion Measure) point is found from a check point pattern at the center of the searching area as shown in (16).

Step 3 : If the search window is equal to (17) then the process stop; otherwise, go to Step 4.

$$[a, b, c, d, e, f] = [\pm 0.16, \pm 0.16, \pm 2, \pm 0.16, \pm 0.16, \pm 2] (17)$$

Step 4 : The search window is reduced by half in all dimensions of the previous search window and a minimum BDM (Block Distortion Measure) point is found from a check point pattern at the center of the new searching area. Go to Step 2.

From [3-4], the total number of the M3SS check points is fixed at $3.65E+3$. Compared with the classical block-based estimation method (translation block-based estimation method) at 0.25 pixel accuracy and $w=9$ (w is searching window), the total number of the M3SS check points has approximately 3 times more than the FS (Full- Search) approach of the COM but the PSNR performance of the M3SS method for GOM is 5-6 dB higher than that of the COM.

4. EXPERIMENTAL RESULT

All methods are implemented in MATLAB and the block size of LR images is fixed at 8×8 (or 16×16 for overlapping block), the search window is 9×9 for classical registration, the search window is 7×7 for proposed registration and 5 frames are used for ML estimation process. The 38th- 42nd frame Susie sequence and the 108th- 112th frame Foreman sequence in QCIF format (176×144), are used in these experiments to reconstruct the high resolution image of the 40th frame of Susie and 110th frame of Foreman, respectively. Both sequences have complex-edge characteristic. Then, to simulate the effect of camera PSF, the images are convolved with a symmetric Gaussian low-pass filter with size of 3×3 and standard deviation of one. The blurred images are subsampled by the factor of two in each direction (88×72) and the blurred subsampled images are corrupted by Gaussian noise.

The criterion for parameter selection in this experiment is to choose parameters which produce both the most visually appealing results and the highest PSNR. Therefore, to ensure fairness, each experiment is repeated several times with different parameters and the best result of each experiment is chosen [16-18].

Table 1: Experimental Result of Susie: COM

Noise Model	Noise Power	PSNR of LR Image (dB)	PSNR of SRR Image (dB)		
			L1	L2	Hampel
AWGN	15	23.7393	26.2371	23.7393	27.6181
	17.5	25.7765	27.16	25.7765	28.5444
	20	27.574	28.8004	27.574	29.418
	22.5	29.0574	29.6625	29.0574	30.0428
	25	30.1487	30.3824	30.1487	30.6286
Poisson		27.9892	28.8819	27.9892	29.4286
S&P	D:0.015	25.521	27.0972	25.521	28.2192
	D:0.010	27.3206	28.2861	27.3206	29.1129
	D:0.005	29.3506	29.7082	29.3506	30.0912
Speckle	V:0.03	23.986	26.7384	23.986	27.9817
	V:0.02	25.272	27.2486	25.272	28.278
	V:0.01	27.5301	28.6916	27.5301	29.3046

The objective of this experiment is to demonstrate the performance of the proposed robust norm regarding to the SRR performance when the Classical Observation Model (COM) and General Observation Model (GOM) are used.

Hence, this section presents the experiments and comparison results obtained by the SRR algorithm using Hampel, L1 and L2 norm with the COM and the GOM at various noise models and noise power. Due to page limitation, PSNR of every case are shown in Table 1-4 and Fig. 3-8 but only some reconstructed results of foreman are shown for visual comparison in Fig. 9.

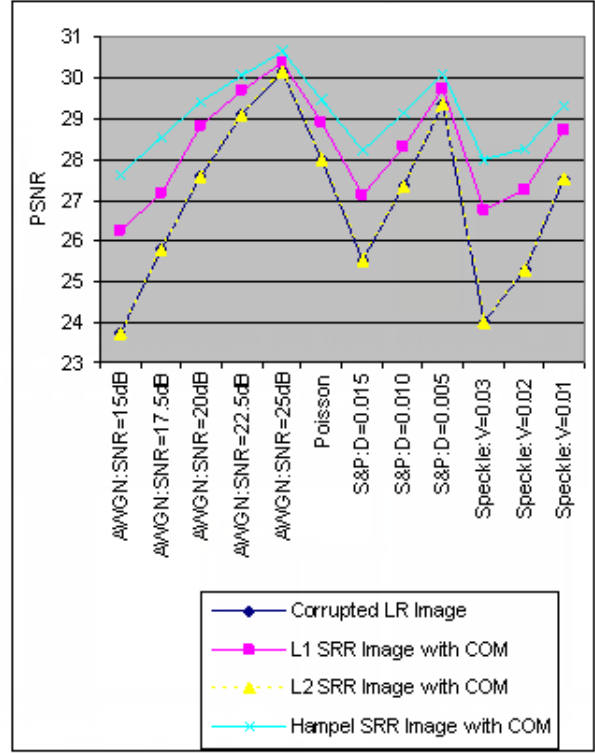


Fig.3: Experimental Result of Susie:COM

Table 2: Experimental Result of Foreman: COM

Noise Model	Noise Power	PSNR of LR Image (dB)	PSNR of SRR Image (dB)		
			L1	L2	Hampel
AWGN	15	20.3124	22.7614	20.3124	23.452
	17.5	22.1395	23.8148	22.1395	24.2431
	20	23.7206	24.7384	23.7206	25.0005
	22.5	24.8508	25.4006	24.8508	25.5716
	25	25.8468	26.0369	25.8468	26.1298
Poisson		25.0577	25.5626	25.0577	25.764
S&P	D:0.015	23.6269	24.5757	23.6269	24.985
	D:0.010	24.6287	25.1489	24.6287	25.4178
	D:0.005	25.5815	25.8052	25.5815	25.946
Speckle	V:0.03	20.557	22.9761	20.557	23.5983
	V:0.02	21.8538	23.7556	21.8538	24.2164
	V:0.01	23.7767	24.8022	23.7767	25.0498

From experimental result, the SRR algorithm using Hampel norm with the proposed registration gives the highest PSNR because these robust estimators are designed to be robust and reject outliers (noise and registration error). Moreover, due to the efficient of the proposed GOM, the SRR algorithm based on Hampel with GOM and COM gave highest PSNR than the other SRR algorithms.

The SRR algorithm using L1 norm with GOM and COM gives the higher PSNR than the SRR algorithm using L2 norm because L2 norm is more sensitive to the outliers such as noise and the registration error

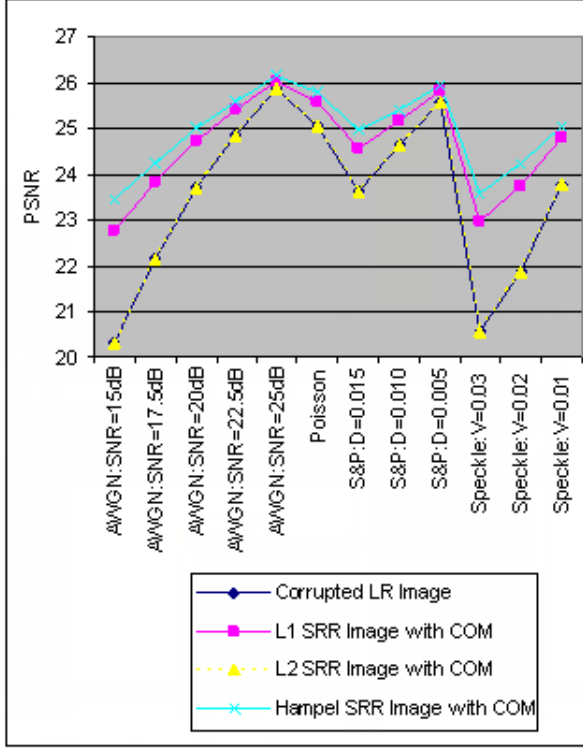


Fig.4: Experimental Result of Foreman:COM

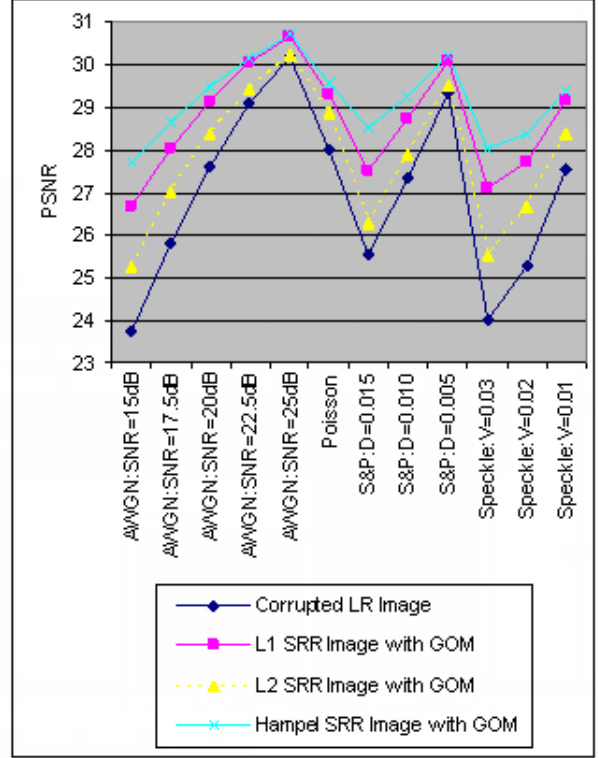


Fig.5: Experimental Result of Susie:GOM

than L1 norm. Moreover, due to the efficient of the proposed general observation model, the SRR algorithm based on L1 norm with general observation model give higher PSNR than the SRR algorithm based on L1 norm with classical observation model.

sult of the SRR algorithm using L2 norm decreases rapidly as shown in experimental results. Moreover, due to the efficiency of the proposed GOM, the SRR algorithm based on L2 norm with GOM gives higher PSNR than the SRR algorithm based on L2 norm with COM.

Table 3: Experimental Result of Susie:GOM

Noise Model	Noise Power	PSNR of LR Image (dB)	PSNR of SRR Image (dB)		
			L1	L2	Hampel
AWGN	15	23.7393	26.6879	25.2707	27.7113
	17.5	25.7765	28.0193	27.0041	28.633
	20	27.574	29.1304	28.3754	29.4776
	22.5	29.0574	30.0186	29.4315	30.1212
	25	30.1487	30.6615	30.2347	30.7068
Poisson		27.9892	29.3107	28.8507	29.5497
S&P	D:0.015	25.521	27.5187	26.2784	28.5041
	D:0.010	27.3206	28.7302	27.8977	29.2558
	D:0.005	29.3506	30.0868	29.5284	30.1961
Speckle	V:0.03	23.986	27.0925	25.5199	28.0071
	V:0.02	25.272	27.7187	26.6633	28.3637
	V:0.01	27.5301	29.1562	28.3942	29.3786

The SRR algorithm using L2 norm with COM and GOM gives the lowest PSNR because L2 norm is more sensitive the outliers such as the noise and registration error. The L2 influence function increases linearly and without bound. Therefore, when the noise power or registration error increases, the PSNR re-

Table 4: Experimental Result of Foreman: GOM

Noise Model	Noise Power	PSNR of LR Image (dB)	PSNR of SRR Image (dB)		
			L1	L2	Hampel
AWGN	15	20.3124	23.1151	21.1894	23.4756
	17.5	22.1395	24.089	22.8283	24.2526
	20	23.7206	24.9608	24.0387	25.0047
	22.5	24.8508	25.5834	24.8508	25.5786
	25	25.8468	26.1473	25.8468	26.1334
Poisson		25.0577	25.7916	25.104	25.764
S&P	D:0.015	23.6269	24.8592	24.2964	25.0201
	D:0.010	24.6287	25.392	24.8303	25.4357
	D:0.005	25.5815	25.9735	25.5815	25.9684
Speckle	V:0.03	20.557	23.3854	21.7708	23.6247
	V:0.02	21.8538	24.0958	22.7284	24.2254
	V:0.01	23.7767	25.0185	24.1172	25.0509

5. CONCLUSIONS

In this paper, we propose a SRR algorithm based on a novel robust estimation norm function with GOM for video enhancement. The proposed SRR

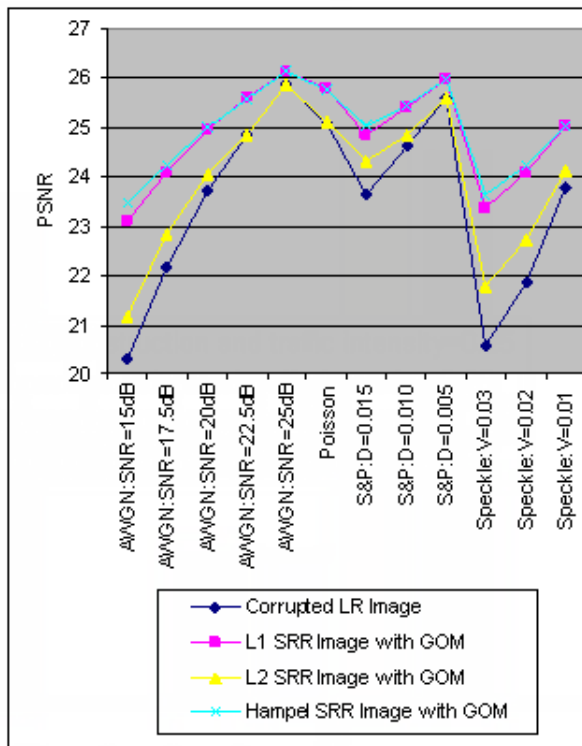


Fig.6: Experimental Result of Foreman:GOM

framework can be applied on video or image sequences corrupted by several noise models and can be applied on the real complex sequence such as Susie and Foreman sequence. Experimental results clearly demonstrated that the proposed algorithm is robust against several noise models (AWGN, Poisson, Salt & Pepper and Speckle noise) at several noise power. The proposed robust algorithm gives higher PSNR and visually better than the algorithm based on L1 and L2 norm in both COM and GOM.

References

- [1] M. K. Ng and N. K. Bose, "Mathematical analysis of super-resolution methodology," *IEEE SP. Magazine*, May. 2003.
- [2] S. C. Park, M. K. Park and M. G. Kang, "Super-Resolution Image Reconstruction : A Technical Over-view," *IEEE SP. Magazine*, May 2003.
- [3] V. Patanavijit and S. Jitapunkul, "An Iterative Super- Resolution Reconstruction of Image Sequences using a Bayesian Approach with BTV Prior and Affine Block-Based Registration," *CRV 2006*, June 2006.
- [4] V. Patanavijit and S. Jitapunkul, "General Observation Model for an Iterative Multiframe Regularized Super-Resolution Reconstruction for Video Enhancement," *IEEE ISPACS 2008*, Thailand, Feb. 2009.
- [5] Rochefort, F. Champagnat, G. L. Besnerais and Jean- Francois Giovannelli, "An Improved Observation Model for Super-Resolution Under Affine Motion," *IEEE Trans. on IP.*, vol. 15 no. 11, Nov. 2006.
- [6] M. Elad and A. Feuer, "Restoration of a Single Super-resolution Image from Several Blurred, Noisy and Un-dersampled Measured Images," *IEEE Trans. on Image Processing*, Vol. 6, Dec. 1997.
- [7] M. Elad and A. Feuer, "Superresolution Restoration of an Image Sequence: Adaptive Filtering Approach," *IEEE Trans. on IP.*, Match 1999.
- [8] R. R. Schultz and R. L. Stevenson, "A Bayesian Approach to Image Expansion for Improved Definition," *IEEE Trans. on IP.*, May 1994.
- [9] R. R. Schultz and R. L. Stevenson, "Extraction of High-Resolution Frames from Video Sequences," *IEEE Transactions on Image Processing*, June 1996.
- [10] M. Elad and A. Feuer, "Restoration of a Single Super-resolution Image from Several Blurred, Noisy and Un-dersampled Measured Images," *IEEE Trans. on Image Processing*, Vol. 6, Dec. 1997.
- [11] M. Elad and A. Feuer, "Super-Resolution Reconstruction of Image Sequences," *IEEE Trans. on PAMI.*, Sep. 1999.
- [12] M. Elad and Y. Hecov Hel-Or, "A Fast Super- Resolution Reconstruction Algorithm for Pure Translational Motion and Common Space-Invariant Blur," *IEEE Trans. on IP.*, 2001.
- [13] Bouman and K. Sauer, "A Generalized Gaussian Image Model for Edge-Preserving MAP Estimation," *IEEE Trans. on IP.*, 2, 3, July 1993 : 293-310.
- [14] M. Elad, "On the Original of the Bilateral Filter and Ways to Improve It," *IEEE Trans. on IP.*, Oct. 2002.
- [15] S. Farsiu, D. Robinson, M. Elad, P. Milanfar, "Advances and Challenges in Super-Resolution," *Wiley Periodicals, Inc.*, 2004
- [16] S. Farsiu, D. Robinson, M. Elad and P. Milanfar, "Fast and Robust Multiframe Super Resolution," *IEEE Trans. on Image Processing*, Oct. 2004.
- [17] S. Farsiu, M. Elad and P. Milanfar, "Multiframe Demosaicing and Super-Resolution of Color Images," *IEEE Trans. on IP*, 2006.
- [18] S. Farsiu, M. Elad and P. Milanfar, "Video-to-Video Dynamic Super-Resolution for Grayscale and Color Sequences," *EURASIP Journal on Applied Signal Processing*, Hindawi Publishing Corporation, 2006.
- [19] M. J. Black, A. Rangarajan, "On The Unification Of Line Processes, Outlier Rejection and Robust Statistics with Applications in Early Vision," *International Journal of Computer Vision* 19, 1, July 1996 : 57-92.
- [20] M. J. Black, G. Sapiro, D. H. Marimont and D.

- Herrger, "Robust Anisotropic Diffusion," *IEEE Trans. on IP.*, 1998.
- [21] V. Patanavijit, "A Robust Iterative Multiframe SRR using Stochastic Regularization Technique based on Hampel Estimation," *ECTI-CON 2008, ECTI Association Thailand*, Krabi, Thailand, 2008.
- [22] V. Patanavijit, "A Robust Iterative Multiframe SRR based on Hampel Stochastic Estimation with Hampel-Tikhonov Regularization," *Proceeding of IEEE 19th International Conference on Pattern Recognition (ICPR 2008)*, Florida, USA, Dec. 2008.
- [23] V. Patanavijit, "Video Enhancement Using A Robust Iterative SRR Based On A Hampel Stochastic Estimation," *ECTI-CON 2009, ECTI Association Thailand*, Pattaya, Thailand, May 2009.

1999 to 2003, he was appointed as the head of Communication Division and the head of the Department, respectively. He also held the position of Associate Dean for Information Technology, Faculty of Engineering from 1993 to 1995. His current research interests are in Image and Video Processing, Speech and Character Recognition, Signal Compression, DSP in Telecommunication, Software Defined Radio, Smart Antenna, and Medical Signal Processing.



Vorapoj Patanavijit received the B.Eng., M.Eng. and Ph.D. degrees from the Department of Electrical Engineering at the Chulalongkorn University, Bangkok, Thailand, in 1994, 1997 and 2007 respectively. He has served as a full-time lecturer at Department of Computer and Network Engineering, Faculty of Engineering, Assumption University since 1998. He works in

the field of signal processing and multidimensional signal processing, specializing, in particular, on Image/Video Reconstruction, SRR (Super-Resolution Reconstruction), Compressive Sensing, Enhancement, Fusion, Denoising, Inverse Problems, Motion Estimation and Registration.



Supatana Auethavekiat received B.E. in electrical engineering from Chulalongkorn University, Thailand in 1996. She received M.E. and Ph.D. in information and communication engineering from the University of Tokyo in 1999 and 2002, respectively. She is current an instructor at Department of Electrical Engineering, Chulalongkorn University. Her research interests are image registration, compressive sensing and video

frame-rate conversion.



Somchai Jitapunkul received the B.Eng. and M.Eng. degrees in Electrical Engineering in 1972 and 1974, respectively from Chulalongkorn University, Thailand. In 1976 and 1978, he received the D.E.A. and Dr. Ing. degrees, respectively, in "Signaux et Systems Spatio-Temporels" from Aix-Marseille University, France. He was appointed as a lecturer in the department of Electrical Engineering at Chulalongkorn University in 1972, Assistant Professor in 1980, and Associate Professor in 1983. In 1993, he was the founder of Digital Signal Processing Research Laboratory where he became the head of this laboratory from 1993 to 1997. From 1997 to 1999 and

1999 to 2003, he was appointed as the head of Communication Division and the head of the Department, respectively. He also held the position of Associate Dean for Information Technology, Faculty of Engineering from 1993 to 1995. His current research interests are in Image and Video Processing, Speech and Character Recognition, Signal Compression, DSP in Telecommunication, Software Defined Radio, Smart Antenna, and Medical Signal Processing.

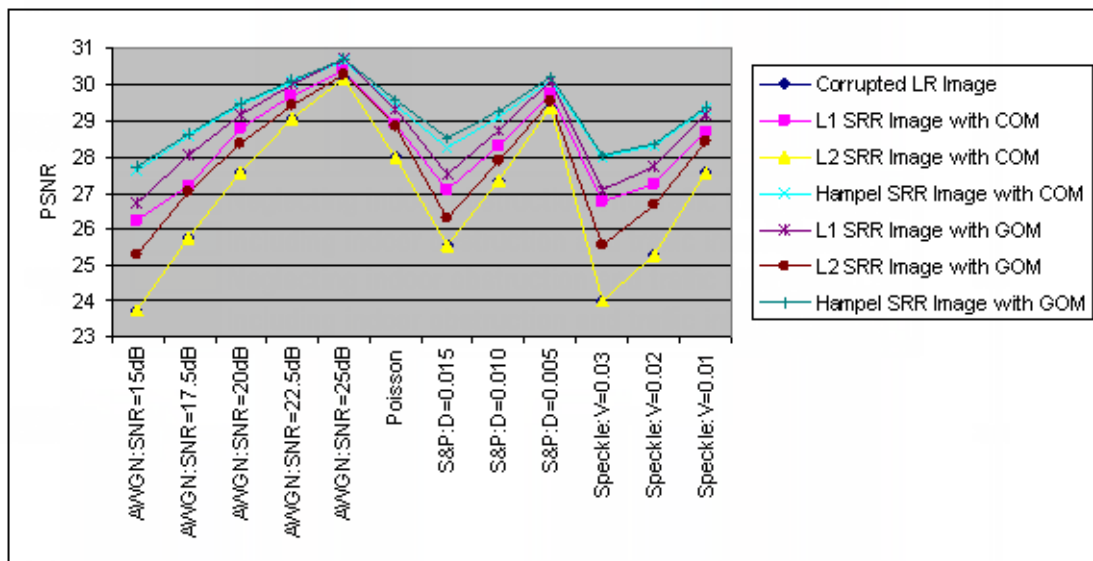


Fig.7: Experimental Result of Susie:COM and GOM

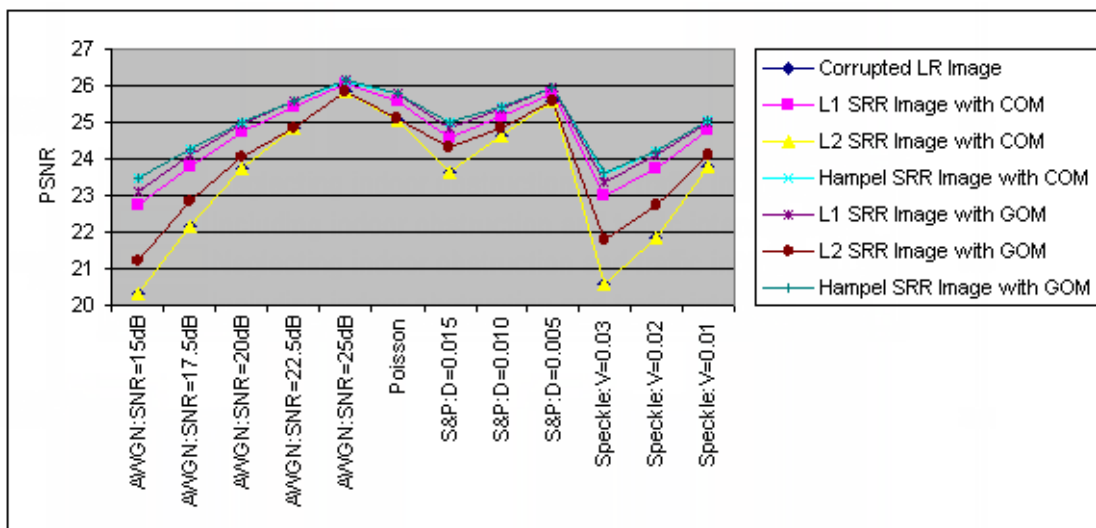


Fig.8: Experimental Result of Foreman:COM and GOM

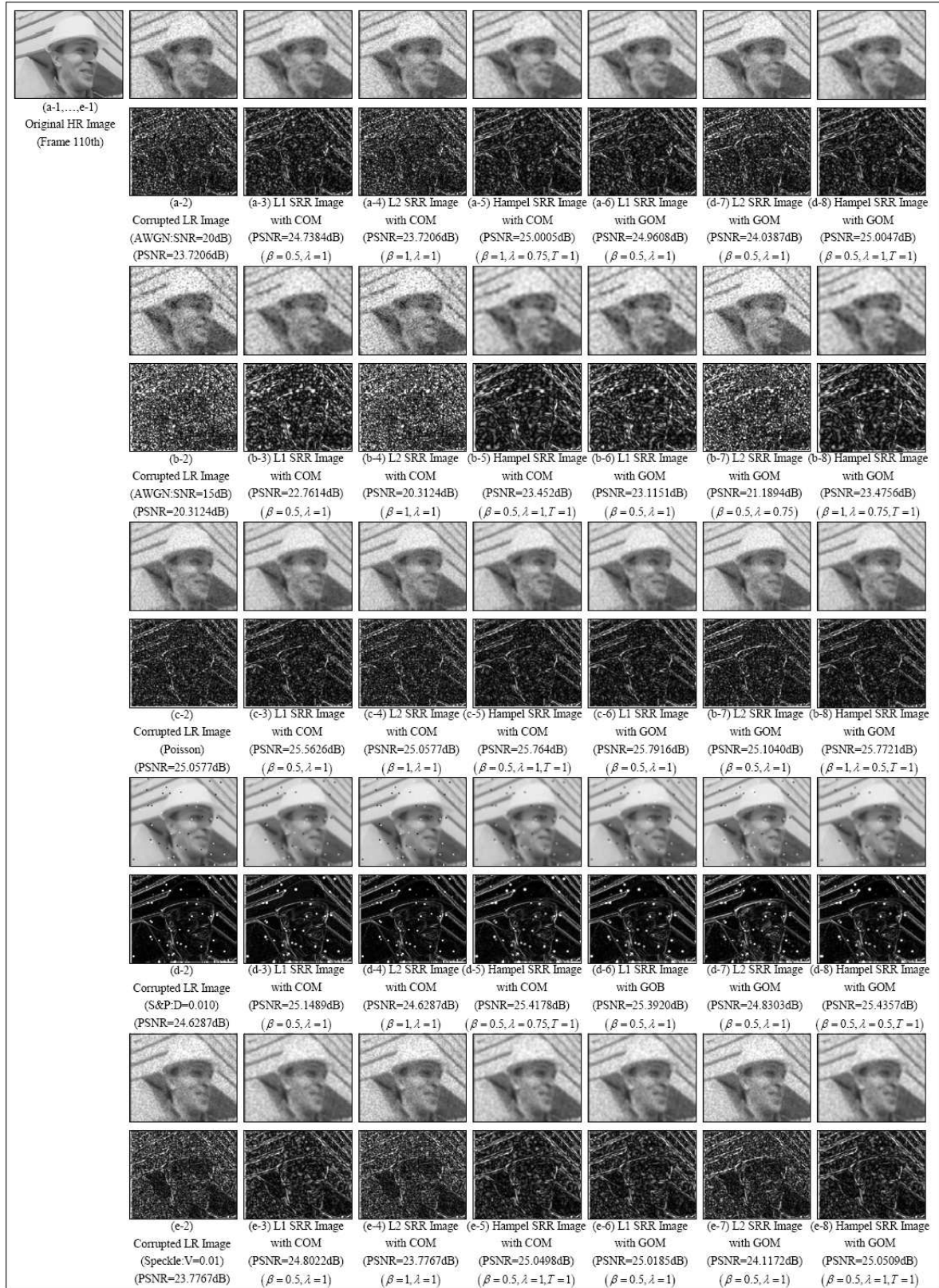


Fig.9: Experimental Result of Foreman:COM and GOM